Date of publication xxxx 00, 0000, date of current version xxxx 00, 0000.

Digital Object Identifier 10.1109/ACCESS.2017.Doi Number

An On-line State of Health Estimation of Lithium-ion Battery using Unscented Particle Filter

Datong Liu[1], Member, IEEE, Xuehao Yin[1], Yuchen Song[1], Student Member, IEEE, Wang Liu[1] and Yu Peng[1], Member, IEEE

[1] Department of Automatic Test and Control, Harbin Institute of Technology, Harbin, 150080, P. R. China

Corresponding author: Datong Liu (e-mail: liudatong@hit.edu.cn).

This work is partly supported by National Natural Science Foundation of China under Grant No. 61571160, 61771157, 61301205

ABSTRACT As one of the key functions in lithium-ion battery management system (BMS), the state-of-health (SOH) estimation is of great significance to ensure the safe and reliable operation and reduce the maintenance cost of the battery energy storage system (BESS). Unscented particle filter (UPF) algorithm is becoming a promising method for battery state estimation since it combines the latest measurement information to give the proposal distribution which is closer to the true posterior distribution. At the same time, UPF algorithm is able to represent the uncertainty involved in the estimation results which makes great significance for battery SOH estimation. On the other hand, it is difficult to measure the battery actual capacity in practice despite the capacity is a direct indicator of battery SOH. In this paper, an on-line health indicator (HI) is extracted from the measurable parameters while battery is working. The mapping model between the extracted HI and battery SOH is established and applied as the observation in the state-space model. An on-line estimator based on UPF algorithm is developed for battery SOH assessment. The maximum estimation error based on battery cycling test data is less than 5%. This indicates that the proposed method has a good adaptability for lithium-ion battery degradation with non-linear and non-Gaussian characteristics. Additionally, the experiments on different types of lithium-ion battery show the good robustness and applicability of this approach.

INDEX TERMS Lithium-ion battery, on-line SOH estimation, health indicator, unscented particle filter

I. Introduction

Lithium-ion batteries have many advantages, such as high output voltage, low self-discharge rate, etc. [1-2]. Thus, they are widely utilized in consumer electronics, electric vehicles, navigation, and aviation applications. Particularly, with the high energy density, lithium-ion battery can significantly reduce the weight and volume of the energy storage system in aerospace applications. Therefore it has become the third generation of satellite power storage batteries [3].

However, the battery performance degrades with the repeatedly charging and discharging. Thus, battery degradation identification, state estimation and prediction, and maintenance optimization have attracted much attention in many different fields including energy, reliability engineering, and aerospace engineering, etc. [4-5].

Indeed, the lithium-ion battery state monitoring, estimation and prediction involving the State-of-Charge (SOC) and State-of-Health (SOH) gradually become the new functional requirements of battery management system (BMS). This paper focuses on the on-line SOH estimation. SOH can represent the battery performance as a measurement that indicates the general health condition of a battery as well as its ability to deliver the specified performance. One of the definitions of SOH is the ratio of the current capacity to the initial capacity. Health state degradation is a long-term variation for a lithium-ion battery [6]. SOH estimation can make some reasonable instructions for battery maintenance and replacement. Accurate estimation results are helpful to ensure the host system running safely, and realize the goal of condition based maintenance (CBM). Moreover, degradation of battery maximum discharge capacity during the long-term operation affects the accuracy of SOC estimation [7], and SOH estimation can solve this problem by updating the battery capacity parameter using the multi-scale joint estimation [8-10].

Capacity is a direct indicator for battery SOH that is applied in most SOH estimation methods. Wu *et al*. [11] acquired the battery capacity through real-time coulomb counting process to achieve SOH estimation. Riviere *et al*. [12] proposed a SOH estimator based on incremental capacity (IC) analysis and a Butterworth filter. Chen *et al.* [13] presented a battery SOH estimation method based on the relationship between Ohmic internal resistance and capacity fade. However, it is hard to take such measurements in on-line applications since lithium-ion batteries may not be fully discharged from the fully charged

state. As a result, the battery capacity cannot be estimated accurately. At the same time, more research efforts have been devoted to construct on-line HIs based on measureable battery parameters. Hu *et al*. [14] proposed a prognostics framework for battery SOH evaluation based on sample entropy of discharging voltage. Liu *et al*. [15-16] constructed a novel HI called the time interval of equal discharging voltage difference (TIEDVD) for battery prognostics.

Data-driven prognostics methods based on testing data samples and monitoring parameters for battery degradation modeling are proved to be effective for battery SOH assessment. For such methods, it is critical to establish a mapping relationship between capacity and measurable physical parameters such as voltage, current, temperature, and time interval. In other words, the complex electrochemical reaction and related principles are not taken into consideration for data-driven methods. In previous literatures, neural network (NN) [17], support vector machine (SVM) [18], relevance vector machine (RVM) [19, 20], and Gaussian process regression (GPR) [21], have been used for battery SOH evaluation. However, such data-driven methods show high dependency on training data sets. When battery is operated in complex conditions, the model may lose its accuracy. Model-based approaches are another kind of SOH estimation methods. The key point of model-based methods is to build the physical model by extracting the internal parameters that are able to characterize dynamic aging and failure process of the battery. Since the model parameters should change with the battery degradation, a variety of filtering methods such as extend Kalman filter (EKF) [22], unscented Kalman filter (UKF) [23-25] and particle filter (PF) [26-29] are applied to adjust the model parameters and hence to track the battery aging process. However, there are some inherent defects for EKF and UKF. Firstly, the methods cannot be well adjusted if the non-linearity of the battery model are serve as the battery ages. Secondly, the system noise and measurement noise must satisfy the Gaussian distribution. However the degradation of lithium-in battery is not in line with these limitations. Therefore, the filtering performance will decrease or even diverge. In comparison, PF algorithm has better ability achieving state estimation with nonlinear and non-Gaussian features. [29]. Xing *et al*. [4] fused an empirical exponential and a polynomial regression model to track battery degradation trend, and the model parameters were adjusted on-line using PF algorithm to implement battery SOH prediction. Saha *et al*. [30] revealed that PF algorithm had better adaptability for battery SOH estimation and prediction when compared with autoregressive integrated moving average (ARMA), EKF, RVM and SVM. PF algorithm is based on Monte Carlo and recursive Bayesian filter methods, and the key concept is to find a collection of random particle sample with associated importance weights to represent the posterior probability density. However, since the standard PF algorithm cannot take account of the newest observation information, all but a few importance weights tend to be zero. This is called particle diversity degradation that reduces the filtering precision and uncertainty representation. To obtain acceptable filtering results and proper probability density distribution, standard PF algorithm requires a massive number of particles which increases the burden of computing. In order to solve these problems, two main strategies can be adopted. One is using resampling techniques, the other is choosing reasonable particle proposal distributions. Although the resampling techniques can solve the lack of particles to some extent, it loses the diversity of particles. Therefore, choosing a reasonable distribution is a promising way to improve the performance of PF algorithm. Unscented particle filter (UPF) is a fusion statistical filtering algorithm that combines the UKF algorithm and PF, and it applies UKF algorithm to give the particle proposal distribution considering the new observation information. Because of the proposal distribution generated by UKF is closer to the true particle posterior distribution, UPF algorithm has a better performance in terms of filtering precision and uncertainty representation compared with PF algorithm, and is becoming an effective method to solve the problems of lithium-ion battery state estimation. More importantly, the number of particles needed in the filtering process is greatly reduced [31]. Miao *et al*. [32-33] proved that UPF algorithm could improve the accuracy of battery SOH prediction, and had better prediction precision and probability density distribution in contrast to PF algorithm.

Despite considerable research efforts have been devoted to lithium-ion battery SOH estimation, there are still some challenging issues. Firstly, data-driven approaches are over-reliance on the training data. If the training data set cannot contain sufficient degradation patterns, the battery SOH cannot be estimated accurately. On the other hand, the parameters of data-driven model are hard to be updated on-line which decrease the capability of the method itself. At the same time, for real applications, it has to be taken into consideration that the degradation features should be extracted from on-line measurable parameters such as voltage and current.

To address the issue of on-line battery SOH estimation, this work extracts the on-line HI by using measurable parameters (voltage, time interval) for working battery. The UPF algorithm is chosen as state filtering method for its better proposal distribution that makes significance for uncertainty representation. The extracted HI are used to construct health model and then SOH is estimated with UPF algorithm. As a result, the on-line battery SOH estimator as well as its confidence interval can be obtained with this fused approach. The on-line SOH estimator this paper proposed fuses the mapping relationship between on-line HI and SOH into the state-space model, and choose the on-line HI as the measurement instead of capacity that achieve the goal of on-line estimation for battery SOH.

The rest of this paper is organized as follows. Section II introduces the methodology of PF algorithm and UPF algorithm. Section III describes the proposed on-line SOH estimation method of lithium-ion battery. Experiments and results analysis are illustrated in section IV. Finally, section V summarizes the conclusion and future work.

II. Methodologies

The state-space equation is a time domain model that

describes the dynamic characteristics of systems, including the state transition and measurement equations which can be expressed as:

$$\mathbf{x}_k = f(\mathbf{x}_{k-1}, \mathbf{v}_{k-1}) \tag{1}$$

$$\mathbf{y}_k = h(\mathbf{x}_k, \boldsymbol{\mu}_k) \tag{2}$$

where $f(\cdot)$ and $h(\cdot)$ represent the state transition and measurement equations respectively. $\mathbf{x}_k$ represents the system state variables, and $\mathbf{y}_k$ is the measurements of the system at time k. $\mathbf{v}_k$ and $\boldsymbol{\mu}_k$ are the system process noise and the measurement noise respectively. They are independent with each other and independent with the system state variables. Both standard PF algorithm and UPF algorithm are designed based on the state-space model.

A. *Particle filter algorithm*

PF algorithm is one of the statistical filtering algorithms that uses Monte Carlo methods to solve the Bayesian estimation problem [34]. It represents the distribution of system state variables by particle collection and can be applied to any form of state-space model, which provides a new idea for solving the probability density distribution of system state estimation. The key of the PF algorithm is to approximate the posterior distribution of the system state variables using a collection of particles $\{\mathbf{x}_k^i\}_{i=1}^N$ with associated weight vector $\{w_k^i\}_{i=1}^N$, and the posterior probability density distribution of the estimated system state variables can be written as

$$p(\mathbf{x}_k \mid \mathbf{y}_{0:k}) \approx \sum_{i=0}^{N} w_k^i \delta(\mathbf{x}_k - \mathbf{x}_k^i) \tag{3}$$

Actually, it is hard to obtain the ideal particle distribution directly from the posterior probability density distribution $p(\mathbf{x}_k \mid \mathbf{y}_{0:k})$. Therefore, it is necessary to find an alternative easy-to-sample particle distribution $q(\mathbf{x}_k \mid \mathbf{y}_{0:k})$ called the proposal distribution to approximate the particle posterior distribution in the standard PF algorithm [30]. The standard PF algorithm is described as follows:

Step 1. Initialization

Set $k = 0$, draw a collection of particles $\{\mathbf{x}_0^i\}_{i=1}^N$ from prior probability distribution $p(\mathbf{x}_0)$ and set all the particle weights to $1/N$. Here, N is the number of particle.

Step 2. Importance sampling

Draw particles $\mathbf{x}_k^i$ from the proposal distribution $q(\mathbf{x}_k^i \mid \mathbf{y}_{0:k})$. In standard PF algorithm, we define $q(\mathbf{x}_k^i \mid \mathbf{y}_{0:k}) = p(\mathbf{x}_k^i \mid \mathbf{y}_{0:k})$.

Step 3. Weight calculation and normalization

Considering the new measured values, calculate the weights of new particles according to the (4), and normalize the weights.

$$w_k^i \propto \frac{p(\mathbf{y}_k \mid \mathbf{x}_k^i) p(\mathbf{x}_k^i \mid \mathbf{x}_{k-1}^i)}{q(\mathbf{x}_k^i \mid \mathbf{x}_{k-1}^i, \mathbf{y}_{1:k})} \tag{4}$$

$$w_k^i = w_k^i \Big/ \sum_{j=1}^{N} w_k^j \tag{5}$$

Step 4. Resampling

Calculate the effective particles with (6),

$$N_{eff} \approx 1 \Big/ \sum_{i=1}^{N} (w_k^i)^2 \tag{6}$$

If the effective sample size N_{eff} is below the given threshold N_{th}, the resampling procedure is conducted according to (7) and (8) for a new collection of particles. Generally, we let $N_{th} = 2/3N$.

$$\mathbf{x}_k^i = \mathbf{x}_k^j, \sum_{j=1}^{N} w_k^j \geq r_k^i \tag{7}$$

$$\overline{w}_k^i = 1/N \tag{8}$$

Step 5. State estimation

Obtain the estimated state variables at time k by the new particles and their corresponding weights.

$$\overline{\mathbf{x}}_k = \sum_{i=1}^{N} \overline{w}_k^i \mathbf{x}_k^i \tag{9}$$

If $k \leq T$ (T is the number of the whole measured values), assume $k = k+1$, turn to *Step 2*. If $k > T$, then the overall estimation algorithm should be ended.

The diversity and effectiveness of particles determine the accuracy and uncertainty representation ability of PF algorithm. However, in the standard PF algorithm, the majority of particle weights tend to be zero after a few steps of iteration, which results in the reduction of the diversity of the particles. In other words, a large number of particles will be unimportant in the filtering process. In order to solve this problem, two methods can be adapted. One is the particle resampling technology and the other is to choose a better particle distribution that has a greater overlap with the true particle posterior distribution. The essence of particle resampling is to discard the particles with lower weights and copy the particles with larger weights, which loses the diversity of particle collection to some extent while solving the problems of particle scarcity. In comparison, choosing a good particle proposal distribution is a more promising way to improve the performance of PF algorithm.

B. *Unscented particle filter algorithm*

UPF algorithm is a converged statistical filtering algorithm that fuses UKF algorithm to generate a particle proposal distribution by taking account of the latest measured values and solves the particle scarcity problems for the standard PF algorithm. Since the particle proposal distribution obtained by UKF algorithm is closer to the true posterior distribution, UPF algorithm has a great advantage in terms of accuracy and the ability of uncertainty representation [31]. UPF algorithm can be divided into two steps: 1) get the particle proposal distribution by the UKF algorithm, 2) use the standard PF algorithm to give the estimation of system state variables and update the corresponding covariance matrix. It is described as follows:

Step 1. Initialization

Randomly generate a collection of particles $\{\mathbf{x}_0^{(i)+}\}$ and the corresponding covariance matrix $\{\mathbf{P}_0^{(i)+}\}$, $i=1,2,...,N$ based on the initial distribution($k=0$), and set

$$\overline{\mathbf{x}}_0^{(i)} = \mathrm{E}[\mathbf{x}_0^{(i)+}] \tag{10}$$

$$\mathbf{P}_0^{(i)+} = \mathrm{E}[(\mathbf{x}_0^{(i)+} - \overline{\mathbf{x}}_0^{(i)})(\mathbf{x}_0^{(i)+} - \overline{\mathbf{x}}_0^{(i)})^{\mathrm{T}}] \tag{11}$$

Step 2. Particle proposal distribution

a) Sigma points generation

Calculate the augmented sigma points for each particle:

$$\mathbf{x}_{k-1}^{(i)a+} = \left[(\mathbf{x}_{k-1}^{(i)+})^{\mathrm{T}} \quad \mathbf{v}_{k-1}^{\mathrm{T}} \quad \boldsymbol{\mu}_{k-1}^{\mathrm{T}}\right]^{\mathrm{T}} \tag{12}$$

$$\mathbf{P}_{k-1}^{(i)a+} = \mathrm{diag}\{\mathbf{P}_{k-1}^{(i)+}, \mathbf{Q}, \mathbf{R}\} \tag{13}$$

$$\boldsymbol{\chi}_{k-1}^{(i)a+} = \left[\mathbf{x}_{k-1}^{(i)a+} \quad \mathbf{x}_{k-1}^{(i)a+} + \gamma\sqrt{\mathbf{P}_{k-1}^{(i)a+}} \quad \mathbf{x}_{k-1}^{(i)a+} - \gamma\sqrt{\mathbf{P}_{k-1}^{(i)a+}}\right] \tag{14}$$

where $\gamma = \sqrt{L+\lambda}$, L is the dimension of the augmented state variables and λ is the composite scaling parameter.

b) Time update

Perform the time update to propagate the particle into the future:

$$\boldsymbol{\chi}_k^{(i)x-} = f(\boldsymbol{\chi}_{k-1}^{(i)x+}, \boldsymbol{\chi}_{k-1}^{(i)v+}) \tag{15}$$

$$\mathbf{x}_k^{(i)-} = \sum_{j=0}^{2L} W_j^{(m)} \boldsymbol{\chi}_{j,k}^{(i)x-} \tag{16}$$

$$\mathbf{P}_k^{(i)-} = \sum_{j=0}^{2L} W_j^{(c)} (\boldsymbol{\chi}_k^{(i)x-} - \mathbf{x}_k^{(i)-})(\boldsymbol{\chi}_k^{(i)x-} - \mathbf{x}_k^{(i)-})^{\mathrm{T}} \tag{17}$$

$$\boldsymbol{\psi}_k^{(i)-} = g(\boldsymbol{\chi}_k^{(i)x-}, \boldsymbol{\chi}_{k-1}^{(i)\mu+}) \tag{18}$$

$$\mathbf{y}_k^{(i)-} = \sum_{j=0}^{2L} W_j^{(m)} \boldsymbol{\psi}_{j,k}^{(i)-} \tag{19}$$

c) Measurement update

Perform the measurement update to incorporate the latest observation information:

$$\mathbf{P}_{y_k,y_k} = \sum_{j=0}^{2L} W_j^{(c)} (\boldsymbol{\psi}_{j,k}^{(i)-} - \mathbf{y}_k^{(i)-})(\boldsymbol{\psi}_{j,k}^{(i)-} - \mathbf{y}_k^{(i)-})^{\mathrm{T}} \tag{20}$$

$$\mathbf{P}_{x_k,y_k} = \sum_{j=0}^{2L} W_j^{(c)} (\boldsymbol{\chi}_{j,k}^{(i)x-} - \mathbf{x}_k^{(i)-})(\boldsymbol{\psi}_{j,k}^{(i)-} - \mathbf{y}_k^{(i)-})^{\mathrm{T}} \tag{21}$$

$$\mathbf{K}_k = \mathbf{P}_{x_k,y_k} \mathbf{P}_{y_k,y_k}^{-1} \tag{22}$$

$$\mathbf{x}_k^{(i)+} = \mathbf{x}_k^{(i)-} + \mathbf{K}_k(\mathbf{y}_k - \mathbf{y}_k^{(i)-}) \tag{23}$$

$$\mathbf{P}_k^{(i)+} = \mathbf{P}_k^{(i)-} - \mathbf{K}_k \mathbf{P}_{y_k,y_k} \mathrm{K}_k^{\mathrm{T}} \tag{24}$$

Step 3. State estimation and covariance matrix update

a) Weight calculation and normalization

Calculate the relative weight of each particle conditioned on the measurement $\mathbf{y}_k$ and normalize the weights:

$$w_k^j \propto \frac{p(\mathbf{y}_k \mid \mathbf{x}_k^{(i)+}) p(\mathbf{x}_k^{(i)+} \mid \mathbf{x}_{k-1}^{(i)+})}{q(\mathbf{x}_k^{(i)+} \mid \mathbf{x}_{k-1}^{(i)+}, \mathbf{y}_{1:k})} \tag{25}$$

$$w_k^i = w_k^j \Big/ \sum_{j=1}^{N} w_k^j \tag{26}$$

b) Resampling

When the effective sample size N_{eff} is below the given threshold N_{th}, we can generate a set of particles $\{\mathbf{x}_k^{(i)+}\}$ and their corresponding covariance matrix $\{\mathbf{P}_k^{(i)+}\}$ on the basis of the relative weight w_k^i by resampling method.

$$\mathbf{x}_k^{(i)+} = \mathbf{x}_k^{(j)+}, \mathbf{P}_k^{(i)+} = \mathbf{P}_k^{(j)+}, \sum_{j=1}^{N} w_k^j \geq r_k^i \tag{27}$$

$$\overline{w}_k^i = 1/N \tag{28}$$

c) State estimation

The system state variables can be given as:

$$\overline{\mathbf{x}}_k = \sum_{i=1}^{N} \mathbf{x}_k^{(i)+} \overline{w}_k^i \tag{29}$$

For $k=1,\ 2\ ,\ \cdots$, repeat the step 2 and step 3 above.

III. Fusion Approach With On-line Health Indicator Extraction For SOH Estimation

A. Overall procedures

In order to realize the on-line estimation of battery SOH, this paper starts from the discharging voltage series and time series that can be monitored directly during the actual operation of batteries, and construct an on-line HI. Taking account of the non-linear and non-Gauss complex features of lithium-ion battery, we achieve the battery SOH estimation based on UPF algorithm, and the on-line estimation framework for battery SOH can be summarized in Fig. 1.

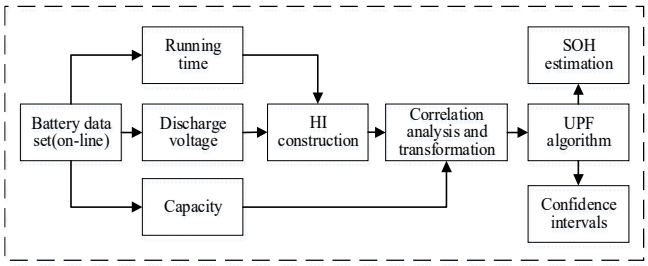

Figure 1. On-line estimation framework for battery SOH

Firstly, the discharging voltage series and time series that can be detected directly are extracted from the battery on-line test dataset. We construct an on-line HI based on these monitored battery parameters, and the correlation between the extracted HI and battery SOH is evaluated and mapped which can be used in the system state-space equation. Then, we apply this mapping relationship into the system state-space equation, realize on-line estimation for battery SOH based on the UPF algorithm, and give the distribution of confidence intervals, with a confidence level of 95%.

B. On-line Health Indicators Extraction and Mapping

Capacity is a direct measurement for battery SOH, but it could not be obtained easily while the battery is working, in other words, capacity cannot be used as the observation of the system state-space equation. Therefore, it is necessary to find the available parameters during battery running, such as voltage, current, time and temperature to construct an efficient HI of battery SOH.

Liu *et al*. [15-16] showed that there were some differences between the discharging voltage cures of each discharging cycle, and the time interval of equal discharging voltage

difference (TIEDVD) could serve as an on-line HI to measure the capacity degradation in each charging and discharging cycle for battery SOH estimation.

The extraction principle of TIEDVD for one charging and discharging cycle is shown in Fig. 2.

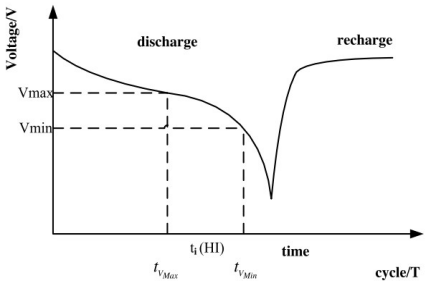

Figure 2. HI extraction with TIEDVD

TIEDVD is an efficient on-line avaliable HI, and the potential degradation based on the TIEDVD index is similar to that of battery capacity. In particular, the on-line HI this paper constructed corresponding to certain charging and discharging cycle is:

$$HI_i = | t_{V_{Max}} - t_{V_{Min}} |, \quad i = 1,2,...,k,... \tag{30}$$

here, $t_{V_{Max}}$ and $t_{V_{Min}}$ are the upper and lower limit voltage sampling time respectively.

The on-line HI series can be expressed as:

$$\mathbf{HI} = \{HI_1, HI_2, ..., HI_k, ...\} \tag{31}$$

The on-line HI can be used as an indirect indicator for battery SOH, and the correlation analysis and transformation relationship between battery SOH and on-line HI is valuable. Based on the experimental results presented in [35], the transformation relationship between battery SOH and TIEDVD can be described as:

$$SOH_i = \beta_0 + \beta_1 HI_i + \beta_2 \ln(HI_i) + \varepsilon_i \tag{32}$$

here, β_1 and β_2 are the coefficients for transformation relationship, β_0 is a constant and ε_i is the error term.

This approximation method applies linear basis expansions, which is one of the extensions of generalized linear regression model. The benefit of this transformation relationship is that one can add smooth functions to describe the linear or non-linear relationship between the two variables.

C. SOH Estimation Based on Fusion UPF

1) Degradation Model and State Transition Equation

The degradation of lithium-ion batteries is a complex electrochemical reaction process, especially the self-charging phenomenon during the charging and discharging cycle makes it hard to establish a suitable model to characterize the overall degradation process well. Fortunately, it is not difficult to see that the overall trend of battery degradation follows the exponential decay. Moreover, Xing *et al*. [4] revealed that the double exponential degradation model could characterize battery degradation process well, and can be written as:

$$SOH_k = a \cdot \exp(b \cdot k) + c \cdot \exp(d \cdot k) \tag{33}$$

where a, b, c and d are the model parameters and k is the cycle number. a and c are related to the internal impendence, b and d are connected with the degradation rate.

Degradation model parameters are chosen as the system state-space variables and the state transition equation can be established as:

$$\mathbf{x}_k = [a_k; b_k; c_k; d_k] \tag{34}$$

$$\begin{cases} a_k = a_{k-1} + v_{a,k-1} & v_a \sim N(0,\ \sigma_a) \\ b_k = b_{k-1} + v_{b,k-1} & v_b \sim N(0,\ \sigma_b) \\ c_k = c_{k-1} + v_{c,k-1} & v_c \sim N(0,\ \sigma_c) \\ d_k = d_{k-1} + v_{d,k-1} & v_d \sim N(0,\ \sigma_d) \end{cases} \tag{35}$$

here, $N(0,\sigma)$ is the Gaussian noise with zero mean and standard deviation σ.

2) Measurement Equation Construction

The measurement equation describes the function relationship between system state variables and observational information, and the on-line HI we constructed is chosen as the measurement of state-space equation. Thus, taking account of battery degradation model and the mapping relationship between on-line HI and SOH, the measurement equation is established as:

$$\begin{cases} SOH_k = a_k \cdot \exp(b_k \cdot k) + c_k \cdot \exp(d_k \cdot k) \\ HI_k = g(SOH_k) + \mu_k \quad \mu_k \sim N(0,\ \sigma_\mu) \end{cases} \tag{36}$$

here, function $g(\cdot)$ represents the transformation relationship between SOH and on-line HI.

3) State Updating and SOH Estimation

The accurate estimation of battery SOH not only depends on the precise degradation model, but also on the optimization and adjustment of model parameters during the degradation process. In this paper, the UPF algorithm are applied to optimize and update the state parameters illustrated in Fig. 3.

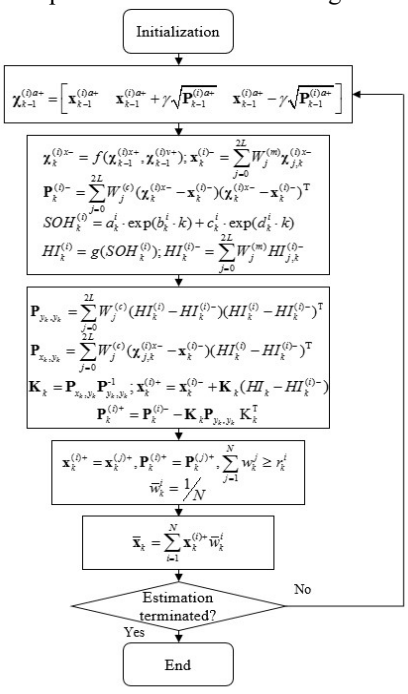

Figure 3. State parameters updating based on UPF algorithm

At cycle k, the estimated SOH collection for each particle can be given by:

$$SOH_k^i = a_k^i \cdot \exp(b_k^i \cdot k) + c_k^i \cdot \exp(d_k^i \cdot k) \quad (37)$$

and the estimated SOH is represented as：

$$SOH_k = \sum_{i=1}^{N} \overline{w}_k^i \cdot SOH_k^i \quad (38)$$

When the SOH is achieved, the estimated confidence interval distribution is given with a confidence level of 95%, and finally form a confidence interval distribution band around the estimated results.

IV. Experiments And Result Discussion

A. Experimental Data Sets

In the experiments, two lithium-ion battery data sets are utilized to verify the proposed methods. Battery B18 is obtained from the data repository of the NASA Ames Prognostics Center of Excellence (PCoE) [36], and CS-36 is from the Center for Advanced Life Cycle Engineering (CALCE) at University of Maryland [1], [4], [37-38].

Battery B18 is a commercial lithium-ion 18650 rechargeable battery with rated capacity 2Ah. The battery is tested in a constant current (CC) mode at 0.75C until the battery voltage reached 4.2V and then charged in a constant voltage (CV) mode until the charge current dropped to 0.01C. Discharge is conducted at a constant current (CC) level of 1C until the battery voltage dropped to 2.5V. Repeated charge and discharge cycles resulted in accelerated aging of the battery. The experiments were stopped when the batteries reached the end-of-life (EOL) with a 30% fade in rated capacity (from 2Ahr to 1.4Ahr).

The rated capacity of battery CS-36 whose rated capacity is 1.1Ah is tested with the charging current 0.5C. While the battery charging voltage reached 4.2V and then charged in a constant voltage mode until the charge current dropped to 0.05A. Discharge is conducted at a constant current level of 1C until the battery voltage dropped to 2.7V.

Different battery samples tested under different charging/discharging conditions can guarantee the general applicability of the proposed methods.

B. Experiment Setting and Evaluation Criteria

Firstly, battery B18 is selected as the experimental sample. Then, battery CS-36 is chosen to conduct the experiments to evaluate the adaptability of the method for different types of battery samples. When the battery SOH is less than 0.8, it is regarded as failure. Thus, in the experiments, only the SOH estimation is analyzed before the battery reaches the failure threshold (SOH=0.8).

In addition, in order to analyze the estimation performance of the proposed method, the PF algorithm is proceeded with the same number of particles ($N=128$) as well as the method comparison. The evaluation indexes include the root mean square error (RMSE), maximum error (ME), maximum relative error (MRE), average error (AE) and average width of confidence interval (AWCI).

(1) Root Mean Square Error (RMSE):

$$RMSE = \sqrt{\frac{\sum_{k=1}^{L} (SOH_{estimation}^k - SOH_{true}^k)^2}{L}} \quad (39)$$

(2) Maximum Error (ME):

$$ME = \max\{(SOH_{estimation}^k - SOH_{true}^k)\}_{k=1}^{L} \quad (40)$$

(3) Maximum Relative Error (MRE):

$$MRE = \max\{\frac{(SOH_{estimation}^k - SOH_{true}^k)}{SOH_{true}^k}\}_{k=1}^{L} \quad (41)$$

(4) Average Error (AE):

$$AE = \frac{\sum_{k=1}^{L} (SOH_{estimation}^k - SOH_{true}^k)}{L} \quad (42)$$

(5) Average Width of Confidence Interval (AWCI):

$$AWCI = \frac{3.92 * \sum_{k=1}^{L} \sigma_k}{L} \quad (43)$$

here, $SOH_{estimation}^k$ and SOH_{true}^k are the estimated value and true value at kth cycle respectively. L is length of iteration and σ_k is the standard deviation of the collection $\{SOH_k^i\}$.

C. Experiments on SOH Estimation and Comparison

1) NASA PCOE BATTERY SOH ESTIMATION

Firstly, the on-line HI is extracted for battery sample B18, and the correlation analysis between the constructed HI and SOH is conducted. Then, the mapping function between on-line and SOH is established for measurement equation and the degradation model is obtained for state transition equation respectively. Finally, the UPF algorithm is applied to optimize the state parameters for SOH estimation and give the confidence interval.

The on-line HI this paper proposed is extracted from the series of discharge voltage serials as well as sample time serials. Figure 4 describes the extracted on-line HI series of battery B18, here $V_{max} = 4.0\text{V}$, and $V_{min} = 3.5\text{V}$.

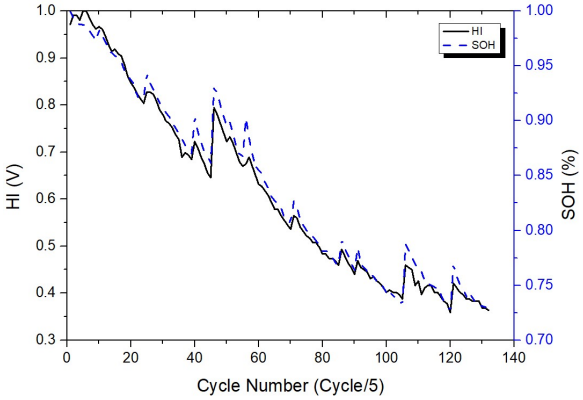

Figure 4. The extracted on-line HI series of battery B18

The correlation analysis curve between on-line HI and battery SOH is shown in Fig. 5. The correlation coefficient $R = 0.991$, which means the extracted on-line HI can be equivalent to the factor characterized the battery SOH.

This article has been accepted for publication in a future issue of this journal, but has not been fully edited. Content may change prior to final publication. Citation information: DOI 10.1109/ACCESS.2018.2854224, IEEE Access

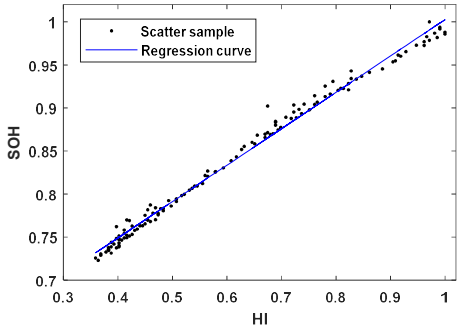

Figure 5. Correlation analysis between on-line HI and SOH for battery B18

The mapped on-line HI obtained with Eq. (32) and the battery SOH are shown in Fig. 6. The coefficients $\beta_0, \beta_1, \beta_2$ are calculated used least square algorithms. The maximum error is 0.0315which indicates the system state-space equation can be established by using the mapping relationship.

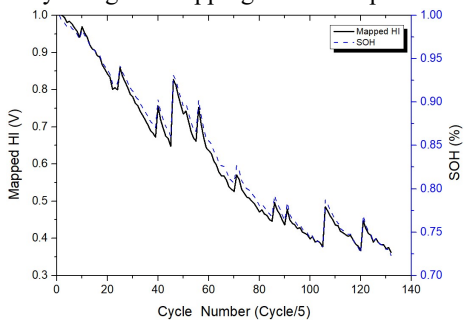

(a) Comparison of mapped HI and SOH

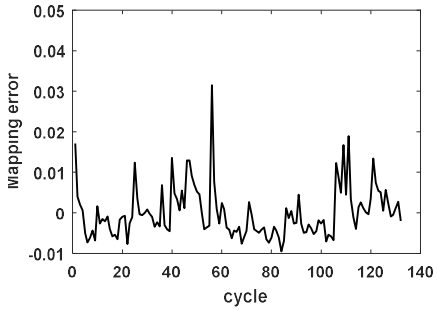

(b) Mapping error

Figure 6. Mapping of on-line HI and SOH for battery B18

The function fitted with double exponential model for battery B18 is shown in Fig. 7. The correlation coefficient $R = 0.9625$, that means the double exponential model has a good ability to characterize the degradation process of battery B18.

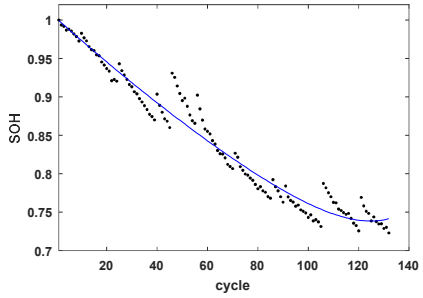

Figure 7. Degradation process fitting for battery B18

In the experiment, the fitting results of the model parameters shown in Table I are selected to initialize the system state variables, and the corresponding standard deviations are calculated by combining the parameter fitting range and rule 3σ.

TABLE I
STATE PARAMETERS INITIALIZATION AND STANDARD DEVIATION FOR BATTERY B18

State Variables	Initial Value	Fitting Range	Standard Deviation
a	1.002	(0.9935, 1.010)	0.0027
b	-0.002918	(-0.003189, -0.002648)	0.00009
c	0.000105	(-4.308e-4, 6.413e-4)	0.00018
d	0.04805	(0.01053, 0.08558)	0.01251

The SOH estimation results in the whole life cycle for battery B18 are shown in Figs 8 - 9.To further evaluate the efficiency of the proposed method, the PF and UPF algorithms are compared in the experiments. Table II shows the quantitative the performance comparison results..

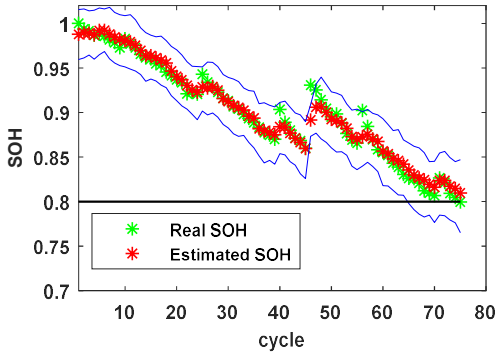

(a) SOH estimation result and its confidence interval

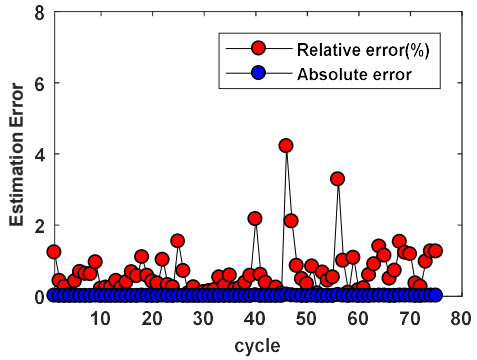

(b) Error of SOH estimation

Figure 8. SOH estimation with basic PF algorithm for battery B18

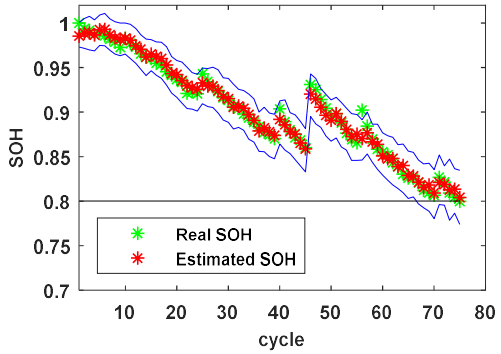

(a) SOH estimation result and its confidence interval

This article has been accepted for publication in a future issue of this journal, but has not been fully edited. Content may change prior to final publication. Citation information: DOI 10.1109/ACCESS.2018.2854224, IEEE Access

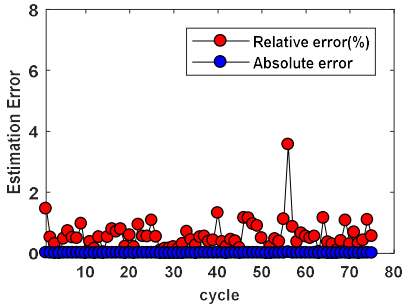

(b) Error of SOH estimation

Figure 9. SOH estimation with UPF algorithm for battery B18

TABLE II
COMPARISON OF SOH ESTIMATION FOR BATTERY B18

Evaluation indexes	PF	UPF
AE	0.0061	0.0050
ME	0.0392	0.0322
MRE	4.2082%	3.5639%
RMSE	0.0012	0.0005
AWCI	0.0606	0.0458

It can been seen that the proposed method has a good performance for SOH estimation of battery B18, and the estimation error is less than 5%. Additionally, the UPF algorithm shows better efficiency in terms of five evaluation indexes when compared with PF algorithm.

2) MARYLAND CALCE BATTERY SOH ESTIMATION

Battery CS-36 is utilized in order to evaluate the adaptability of different types of batteries. The constructed HI and the true SOH for battery CS-36 are shown in Fig. 10.

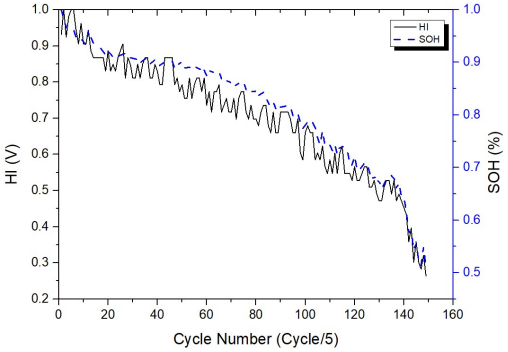

Figure 10. The extracted on-line HI series of battery CS-36

The On-line HI against SOH of CS-36 is shown as Fig. 11. The correlation of on-line HI and SOH is higher than 0.96. In other words, the variation of battery SOH can be presented by the proposed HI.

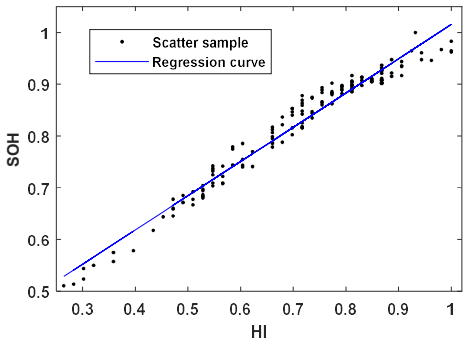

Figure 11. Correlation analysis between on-line HI and SOH for battery CS-36

The mapped on-line HI and battery SOH are shown as Fig. 12. The maximum error is 0.0436 which indicates the system state-space equation can be established with this mapping relationship.

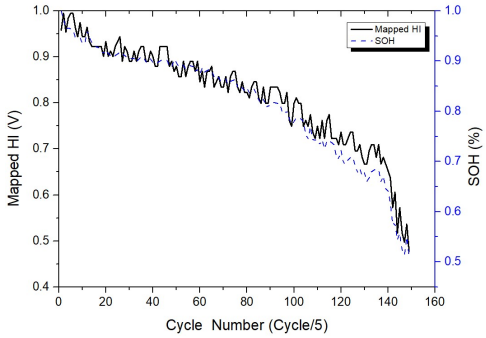

(a) Comparison of mapped HI and SOH

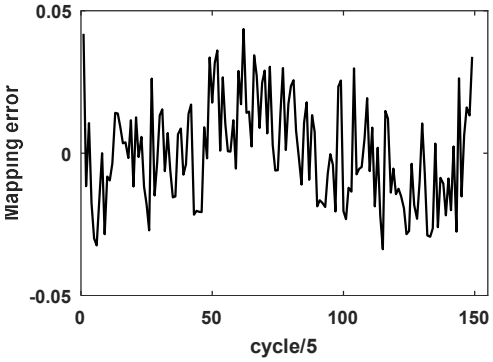

(b) Mapping error

Figure 12. Mapping of on-line HI and SOH for battery CS-36

The double exponential degradation model for battery CS-36 is fitted as Fig. 13. The correlation coefficient $R = 0.9811$, meaning the degradation model can characterize the degradation process of battery CS-36 well. The state parameters initialization and their standard deviations are listed in Table III.

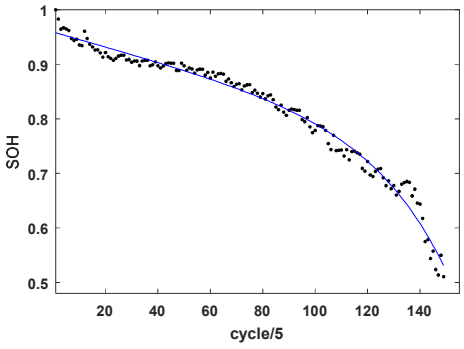

Figure 13. Degradation process fitting for battery CS-36

TABLE III
STATE PARAMETERS INITIALIZATION AND STANDARD DEVIATION FOR BATTERY CS-36

State Variables	Initial Value	Fitting Range	Standard Deviation
a	-0.001432	(-0.003069, 0.000205)	0.000546
b	0.03466	(0.0275, 0.0418)	0.00238
c	0.9608	(0.954, 0.968)	0.0023
d	-0.001386	(-0.00166, -0.00111)	0.000092

The SOH estimation results for battery CS-36 are shown in Figs. 14-15. The PF and UPF algorithms are evaluated and

compared in the experiments, and the quantitative performance comparison are given in Table IV.

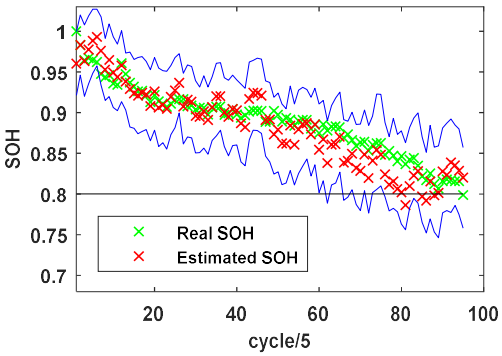

(a) SOH estimation result and its confidence interval

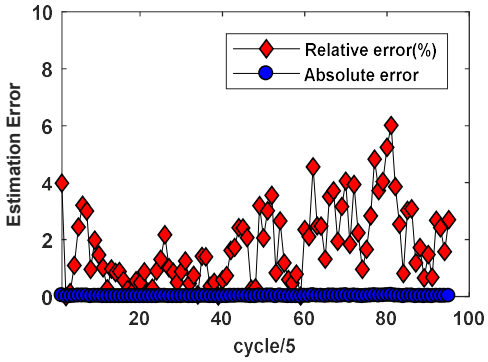

(b) Error of SOH estimation

Figure 14. SOH estimation with UPF algorithm for battery CS-36

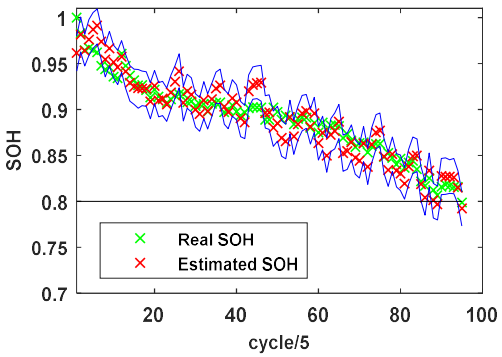

(a) SOH estimation result and its confidence interval

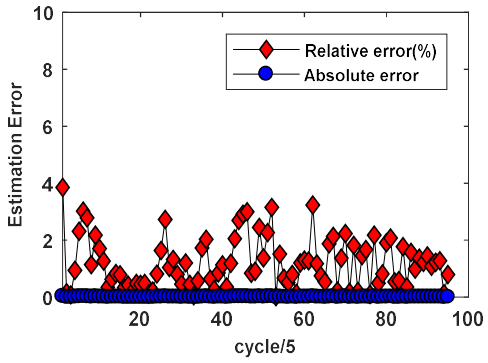

(b) Error of SOH estimation

Figure 15. SOH estimation with UPF algorithm for battery CS-36

TABLE IV
COMPARISON OF SOH ESTIMATION FOR BATTERY CS-36

Evaluation indexes	PF	UPF
AE	0.0155	0.0107
ME	0.0503	0.0385
MRE	6.0111%	3.8483%
RMSE	0.0022	0.00065
AWCI	0.0935	0.0374

Similarly, the proposed method still has a good performance for SOH estimation of battery CS-36. Especially, compared with PF algorithm, the UPF algorithm shows better abilities of average width confidence interval.

D. Experimental Discussion

From Tables II and IV, it can be obtained that PF methods have good performance in battery SOH estimation, and the maximum relative error of SOH estimation is within 10%. This indicates that the method is suitable for non-linear and Non-Gaussian system such as lithium-ion battery. In addition, the proposed UPF algorithm combining degradation model and on-line HI is superior to the basic PF algorithm. And the maximum relative error can be reduced to within 5%, especially in the uncertainty representation of SOH estimation, the 95% confidence interval of UPF algorithm is much more convergent, and contains most of the SOH actual value, which shows that the estimation results have high precision and accuracy. Moreover, the proposed method has good adaptability on different types of lithium-ion batteries, which shows that the method has good robustness.

V. Conclusions

In this paper, an on-line estimation method for lithium-ion battery SOH based on UPF algorithm is proposed. Since the battery actual capacity is hard to be measured when battery is actually operated, this paper first construct an on-line measurable health indicator, namely, TIEDVD from discharging voltage and time measurements. The correlation between this HI and SOH is higher than 0.95 and the mapping error is less than 0.05 that could be a perfect replacement for SOH estimation. The mapping relationship between extracted HI and battery SOH is established and then applied to the system state-space equation. The double exponential degradation model is built, and the UPF algorithm is employed to adjust the model parameters in real time. The experiments validate the on-line estimation method The results indicate that SOH estimation based on UPF algorithm not only has high precision, but also provides great robustness to suppress model parameter perturbations. Compared with PF algorithm, the proposed method has better performance in terms of the average error, maximum error, maximum relative error, root mean square error and average width of confidence interval. Meanwhile, the UPF algorithm can effectively adapt to lithium-ion battery with non-linear and non-Gaussian characteristics and owns the ability of uncertainty representation that is of great significance for the health management of lithium-ion battery. Additionally, the proposed SOH estimation approach estimates the battery health state based on the on-line

measurable parameters instead of capacity. Therefore, this SOH estimator can be utilized in real lithium-ion battery applications.

However, it is much more complex when battery is operated in the dynamic conditions. This challenging issue will be researched in the future. At the same time, the proposed framework will also be optimized for embedded platforms which will make the proposed framework more applicable.

REFERENCES

[1] W. He, N. Williard, M. Osterman, and M. Pecht, "Prognostics of lithium-ion batteries based on dempster-shafer theory and the bayesian monte carlo method," Journal of Power Sources, vol. 196, no. 23, pp. 10314-10 321, 2011.

[2] M. Dalal, J. Ma, and D. He, "Lithium-ion battery life prognostic health management system using particle filtering framework," Journal of Risk and Reliability, vol. 225, no. 1, pp. 81-90, 2015.

[3] Y. Song, D. Liu, C. Yang and Y. Peng, "Data-driven hybrid remaining useful life estimation approach for spacecraft lithium-ion battery", Microelectronic Reliability., vol. 75, pp. 142-153, 2017.

[4] Y. Xing, E. W. M. Ma, K. L. Tsui, and M. Pecht, "An ensemble model for predicting the remaining useful performance of lithium-ion batteries," Microelectronics Reliability, vol. 53, no. 6, pp. 811-820, 2013.

[5] J. Liu, W. Wang, and F. Golnaraghi, "An enhanced diagnostic scheme for bearing condition monitoring," IEEE Transactions on Instrumentation and Measurement, vol. 59, no. 2, pp. 309-321, 2010.

[6] A. P. Schmidt, M. Bitzer, rpd W. Imre, and L. Guzzella, "Model-based distinction and quantification of capacity loss and rate capability fade in li-ion batteries," Journal of Power Sources, vol. 195, no. 22, pp. 7634-7638, 2010.

[7] Y. Wang, C. Zhang, and Z. Chen, "A method for state-of-charge estimation of lifepo 4 batteries at dynamic currents and temperatures using particle filter," Journal of Power Sources, vol. 279, no. ISSN, pp. 306-311, 2015.

[8] C. Hu, B. D. Youn, and J. Chung, "A multiscale framework with extended kalman filter for lithium-ion battery soc and capacity estimation," Applied Energy, vol. 92, no. 4, pp. 694-704, 2012.

[9] R. Xiong, F. Sun, Z. Chen, and H. He, "A data-driven multi-scale extended kalman filtering based parameter and state estimation approach of lithium-ion olymer battery in electric vehicles," Applied Energy, vol. 113, no. 1, pp. 463-476, 2014.

[10] Y. Hua, A. Cordoba-Arenas, N. Warner, and G. Rizzoni, "A multi time-scale state-of-charge and state-of-health estimation framework using nonlinear predictive filter for lithium-ion battery pack with passive balance control," Journal of Power Sources, vol. 280, pp. 293-312, 2015.

[11] T. H. Wu, J. K. Wang, C. S. Moo, and A. Kawamura, "State-of-charge and state-of-health estimating method for lithiumion batteries," in Control and Modeling for Power Electronics, pp. 1-6, 2016.

[12] E. Riviere, P. Venet, A. Sari, F. Meniere, and Y. Bultel, (2015, October). "LiFePO4 battery state of health online estimation using electric vehicle embedded incremental capacity analysis," in Vehicle Power and Propulsion Conference, pp. 1-6, 2015.

[13] L. Chen, Z. L, W. Lin, J. Li, and H. Pan, "A new state-of-health estimation method for lithium-ion batteries through the intrinsic relationship between ohmic internal resistance and capacity," Measurement, vol. 116, pp. 586-595, 2018.

[14] X. Hu, J. Jiang, D. Cao and B. Egardt, Battery health prognosis for electricvehicles using sample entropy and sparse bayesian predictive modeling, IEEE Transactions on Industrial Electronics vol. 633, no.4, pp. 2645-2656, 2016.

[15] D. Liu, H. Wang, Y. Peng, W. Xie, and H. Liao, "Satellite lithium-ion battery remaining cycle life prediction with novel indirect health indicator extraction," Energies, vol. 6, no. 8, pp. 3654-3668, 2013.

[16] D. Liu, J. Zhou, H. Liao, Y. Peng, and X. Peng, "A health indicator extraction and optimization framework for lithium-ion battery degradation modeling and prognostics," IEEE Transactions on Systems Man and Cybernetics Systems, vol. 45, no. 6, pp. 915-928, 2015.

[17] A. Eddahech, O. Briat, N. Bertrand, J. Y. Deltage and J. M. Vinassa, "Behavior and state-of-health monitoring of li-ion batteries using impedance spectroscopy and recurrent neural networks," International Journal of Electrical Power and Energy Systems, vol. 42, no. 1, pp. 487-494, 2012.

[18] C. Hu, G. Jain, C. Schmidt, C. Strief and M. Sullivan, Online estimation of lithium-ion battery capacity using sparse bayesian learning, Journal of Power Sources vol. 289, pp. 105-113, 2015.

[19] D. Liu, J. Zhou, D. Pan, Y. Peng and X. Peng, "Lithium-ion battery remaining useful life estimation with an optimized relevance vector machine algorithm with incremental learning," Measurement, vol. 63, pp. 143-151, 2015.

[20] Y. Song, D. Liu, Y. Hou, J. Yu and Y. Peng, "Satellite lithium-ion battery remaining useful life estimation with an iterative updated rvm fused with the kf algorithm", Chinese Journal of Aeronautics, vol. 31 pp. 31-40, 2018.

[21] D. Liu, J. Pang, J. Zhou, Y. Peng and M. Pecht, "Prognostics for state of health estimation of lithium-ion batteries based on combination gaussian process functional regression," Microelectronics Reliability, vol. 53, no. 6, pp. 832-839, 2013.

[22] J. Kim and B. H. Cho, "State-of-charge estimation and state-of-health prediction of a li-ion degraded battery based on an ekf combined with a per-unit system," IEEE Transactions on Vehicular Technology, vol. 60, no. 9, pp. 4249-4260, 2011.

[23] Z. P. Chen and Q. T. Wang, "The application of ukf algorithm for 18650-type lithium battery soh estimation," Applied Mechanics and Materials, vol. 519-520, pp. 1079-1084, 2014.

[24] S. L. Liu, N. X. Cui, C. H. Zhang, and S. University, "State of health estimation of lithium-ion battery based on aukf," Power Electronics, 2017.

[25] Q. Wang, Y. Jiang, and Y. Lu, "State of health estimation for lithium-ion battery based on d-ukf," International Journal of Hybrid Information Technology, vol. 8, 2015.

[26] R. Xiong, Y. Zhang, H. He, X. Zhou and M. G. Pecht, A double-scale, particle-fltering, energy state prediction algorithm for lithium-ion batteries, IEEE Transactions on Industrial Electronics vol. 65 no. 2, 1526-1538, 2018.

[27] F. Li and J. Xu, "A new prognostics method for state of health estimation of lithium-ion batteries based on a mixture of gaussian process models and particle filter," Microelectronics Reliability, vol. 55, no. 7, pp. 1035-1045, 2015.

[28] J. Li, L. Wang, L. Chao, L. Zhang and H. Wang, "Discharge capacity estimation for li-ion batteries based on particle filter under multi-operating conditions," Energy, vol. 86, pp. 638-648, 2015.

[29] H. Dong, X. Jin, Y. Lou and C. Wang, "Lithium-ion battery state of health monitoring and remaining useful life prediction based on support vector regression-particle filter," Journal of Power Sources, vol. 271, pp. 114-123, 2014.

[30] G. Dong, Z. Chen, J. Wei, C. Zhang and P. Wang, "An online model-based method for state of energy estimation of lithium-ion batteries using dual filters," Journal of Power Sources, vol. 301, pp. 277-286, 2016.

[31] B. Saha, G. Kai and J. Christophersen, "Comparison of prognostic algorithms for estimating remaining useful life of batteries," Transactions of the Institute of Measurement and Control, vol. 31, no. 3, pp. 293-308, 2009.

[32] Y. He, X. T. Liu, C. B. Zhang and Z. H. Chen, "A new model for state-of-charge (soc) estimation for high-power li-ion batteries," Applied Energy, vol. 101, no. 1, pp. 808-814, 2013.

[33] Q. Miao, L. Xie, H. Cui, W. Liang and M. Pecht, "Remaining useful life prediction of lithium-ion battery with unscented particle filter technique," Microelectronics Reliability, vol. 53, no. 6, pp. 805-810, 2013.

[34] X. Zhang, Q. Miao and Z. Liu, "Remaining useful life prediction of lithium-ion battery using an improved upf method based on mcmc," Microelectronics Reliability, vol. 75, pp. 288-295, 2017.

[35] N. J. Gordon, D. J. Salmond, and A. F. M. Smith, "Novel approach to nonlinear/non-gaussian bayesian state estimation," IEE Proceedings F - Radar and Signal Processing, vol. 140, no. 2, pp. 107-113, 2002.

[36] D. Liu, W. Xie, H. Liao, and Y. Peng, "An integrated probabilistic approach to lithium-ion battery remaining useful life estimation," IEEE Transactions on Instrumentation and Measurement, vol. 64, no. 3, pp. 660-670, 2015.

[37] B. Saha and K. Goebel, *Battery Data Set, NASA Ames Prognostics Data Repository*, NASA Ames, Moffett Field, CA, USA, 2007. [Online]. Available: http://ti.arc.nasa.gov/project/prognostic-data-repository

[38] D. Wang, Q. Miao, and M. Pecht, "Prognostics of lithium-ion batteries based on relevance vectors and a conditional three-parameter capacity degradation model," Journal of Power Sources, vol. 239, no. 10, pp. 253-264, 2013.

[39] W. He, N. Williard, M. Osterman, and M. Pecht, "Prognostics of lithium-ion batteries using extended Kalman filtering," in Proc. Int. Microelectron. Assembly Packag. Soc. (IMAPS) Adv. Technol. Workshop High Rel. Microelectron. Military Appl., Fountain Hills, AZ, USA, pp. 1–4, 2011.